Antimicrobial Behavior of Semifluorinated-Quaternized Triblock Copolymers against Airborne and Marine Microorganisms

Daewon Park,[†] John A. Finlay,[‡] Rebekah J. Ward,[§] Craig J. Weinman,[†] Sitaraman Krishnan,[†,||] Marvin Paik,[†] Karen E. Sohn,[⊥] Maureen E. Callow,[‡] James A. Callow,[‡] Dale L. Handlin,[#] Carl L. Willis,[#] Daniel A. Fischer,[▽] Esther R. Angert,[§] Edward J. Kramer,[⊥] and Christopher K. Ober*[,†]

Department of Materials Science & Engineering and Department of Microbiology, Cornell University, Ithaca, New York 14853, School of Biosciences, The University of Birmingham, Birmingham B15 2TT, United Kingdom, Department of Chemical and Biomolecular Engineering, Clarkson University, Potsdam, New York 13699, Department of Materials, University of California, Santa Barbara, California 93106, KRATON Polymers, Houston, TX 77082, and National Institute of Standards and Technology, Gaithersburg, Maryland 20899

ABSTRACT Semifluorinated-quaternized triblock copolymers (SQTCs) were synthesized by chemical modification of polystyrene-*block*-poly(ethylene-*ran*-butylene)-*block*-polyisoprene ABC triblock copolymers. Surface characterization of the polymers was performed by X-ray photoelectron spectroscopy (XPS) and near-edge X-ray absorption fine structure (NEXAFS) analysis. The surface of the SQTC showed very high antibacterial activity against the airborne bacterium *Staphylococcus aureus* with >99 % inhibition of growth. In contrast in marine fouling assays, zoospores of the green alga *Ulva* settled on the SQTC, which can be attributed to the positively charged surface. The adhesion strength of sporelings (young plants) of *Ulva* and *Navicula* diatoms (a unicellular alga) was high. The SQTC did not show marked algicidal activity.

KEYWORDS: semifluorinated-quaternized • ABC triblock copolymer • antibacterial • marine fouling • Ulva • Navicula

INTRODUCTION

Treatments that kill or suppress the growth of bacteria such as heat, chlorine, and antibiotic drugs are classified as antibacterial. In general, antibacterial agents such as bactericides or disinfectants are low-molecular-weight compounds. A specific class of bactericides, low-molecular-weight quaternary ammonium salts possessing at least one alkyl group, is able to kill bacteria by interacting with the cell membrane. Unfortunately, most of these molecules are toxic to the environment, and their effectiveness is short-lived (1−3). Additionally, after years of overuse and misuse of antibacterial compounds, bacteria have developed resistance against antibacterial agents. The development of resistant bacteria has arguably become a global health crisis (4).

Because the polymeric materials widely used in food packaging, textiles, and medical devices can be easily colonized by bacteria or other microorganisms capable of causing severe transmitted diseases, the use of synthetic polymers containing biocidal compounds has steadily increased. Antibacterial polymers have the advantage that they show enhanced antibacterial activity, reduced residual toxicity, increased efficiency and selectivity, and prolonged lifetime. Therefore, investigation of polymeric antimicrobial agents represents a new and important direction that has developed in the field of antimicrobial agents (5, 6). The use of nonleaching antibacterial polymeric surfaces, with antibacterial agents permanently grafted to the surface through covalent bonding, is an attractive strategy. During the last two decades, there has been increased effort to synthesize antibacterial polymeric systems capable of preventing bacterial infections. One method to control bacterial infection is to introduce antibacterial agents within the polymers. This can be achieved by either physical entrapment of the agents in a polymer matrix or grafting the agents onto the surface of polymers (7−10). The other method is to use polymeric materials in which the active moieties are either bound to the polymer backbone or present as pendent groups on the polymer chain (11−18).

Among these polymeric antibacterial materials, there has been significant study concerning the preparation of per-

* Corresponding author.
Received for review October 31, 2009 and accepted January 25, 2010
† Department of Materials Science & Engineering, Cornell University.
‡ The University of Birmingham.
§ Department of Microbiology, Cornell University.
|| Clarkson University.
⊥ University of California.
KRATON Polymers.
▽ National Institute of Standards and Technology.
DOI: 10.1021/am900748v

manent antibacterial surfaces through covalent coupling of poly(quaternary ammonium) compounds (12, 14, 16, 18−20). Quaternary ammonium compounds (QACs) have some advantages over other antibacterial agents. This includes excellent cell membrane penetration properties, low mammalian toxicity and sensitivity, good environmental stability, low corrosivity, and extended residence time and biological activity (13, 21). Although the exact mechanism of the antimicrobial action of QACs is still unclear, it is mostly attributed to their ability to increase cell permeability and disrupt the cell membrane. To be compatible with the bilayer of the outer cell membranes, at least one of the organic substituents should be a long alkyl chain to provide a hydrophobic segment (22). The generally accepted mechanism of action is that the cationic sites of the QACs are adsorbed onto anionic sites of the cell-wall surface by electrostatic interaction, and then a significant lipophilic component promotes diffusion through the cell wall and binds to the cell membrane. Acting as a surfactant, the long alkyl chains are able to disrupt the cytoplasmic membrane and cause the release of electrolytes and nucleic materials which results in the death of the cells (23−25). Recently, several research groups have reported that polymeric QACs such as *N*-alkylated pyridinium polymers (26, 27), *N*-alkylated polyethylenimine (28), and semifluorinated pyridinium polymers (14) are highly bactericidal against *Staphylococcus aureus*, causing rupture of the cell membrane and death rather than simply inhibiting cell growth on the surfaces.

Biofouling due to the colonization of submerged surfaces by aquatic organisms in its early stages is similar to bacterial colonization and is a major problem for all marine industries. Fouling on surfaces promotes corrosion, causes a decrease in hydrodynamic efficiency, results in transport of introduced pests, and leads to many other problems worldwide (29, 30). Currently, the major strategy for combating fouling is via the use of biocidal copper laden antifouling paints (31). From an environmental perspective, non-biocidal technologies are preferred (32). Many researchers have prepared foul-release coatings that minimize the adhesion of fouling organisms including siloxanes (33−35) and fluoropolymers (36−38). Majumdar et al. (39) tethered quaternary ammonium salt moieties into a polysiloxane matrix. The development of a marine bacterial biofim was inhibited by the incorporation of C18 quaternary ammonium moieties and although the surfaces were not antifouling towards the growth of the alga *Ulva*, the release of young plants was enhanced (39).

In this study, we report the development of nontoxic antimicrobial semifluorinated-quaternized triblock copolymers (SQTCs) from polystyrene-*b*-poly(ethylene-*ran*-butylene)-*b*-polyisoprene, PS-*b*-P(E/B)-*b*-PI, ABC triblock copolymer. The triblock copolymer is mechanically locked to the base layer consisting of low modulus thermoplastic polystyrene-*b*-poly(ethylene-*ran*-butylene)-*b*-polystyrene (SEBS) that is utilized to control the mechanical properties of the coating system. The nonpolar nature and rodlike conformation of the fluoroalkyl groups may be instrumental in the higher antibacterial activity of the surfaces of fluorinated-quaternized polymers (14). Thus our goal was to use these surfaces to both improve anti-microbial activity and to serve as antifouling materials. In order to characterize the chemical compositions of the polymeric coating surfaces, near-edge X-ray absorption fine structure (NEXAFS) analysis and X-ray photoelectron spectroscopy (XPS) measurements were performed. Finally, we describe the antibacterial activities of these materials against an airborne Gram-positive bacterium *S. aureus* and report on our testing of these surfaces to resist and release fouling by algae, specifically the green macroalga *Ulva linza* and the diatom *Navicula*. The rationale for the algal assays was based on the premise that the settlement of cells, spores, or larvae of higher organisms may be moderated using tethered, contact-active biocide moieties may delay the fouling process.

EXPERIMENTAL SECTION

Materials. Perfluorooctyliodide and sodium bis(2-methoxyethoxy)aluminum hydride solution (Red-Al) were purchased from Fluka and used as received. 5-Hexen-1-ol, 2,2′-azobisisobutyronitrile (AIBN), sodium bis(2-methoxyethoxy)aluminum hydride, *N,N*-dimethylformamide (DMF), 1-methyl-2-pyrrolidinone (NMP), tetrahydrofuran (THF), methylene chloride, 3-(dimethylamino)-1-propylamine (DMAPA), and 1-bromohexane (H6Br) were purchased from Aldrich and used as received. Triphenylphosphine (TPP), carbon tetrabromide (CBr_4), potassium carbonate, and *m*-chloroperoxybenzoic acid (*m*CPBA) were purchased from Sigma-Aldrich. The polystyrene$_{8k}$-*block*-poly(ethylene-*ran*-butylene)$_{25k}$-*block*-polyisoprene$_{20k}$, PS-*b*-P(E/B)-*b*-PI, triblock copolymer, with PS, P(E/B), and PI block molecular weights of 8, 25, and 20 kDa, respectively, was produced using anionic polymerization by Kraton Polymers. All other chemicals were purchased from Sigma-Aldrich and used without further purification.

Synthesis of Semifluorinated Hexylbromide (F8H6Br). Perfluorooctyliodide (30 g, 55 mmol) and 5-hexen-1-ol (6.61 g, 66 mmol) were mixed in a 100 mL round bottom flask. AIBN (0.45 g, 2.75 mmol) was added and the reaction was performed for 2 h at 80 °C under a nitrogen atmosphere. The crude product was cooled to room temperature and semifluorinated iodohexanol (F8H6IOH) was recovered by crystallization in toluene/hexane (30/120 mL) mixture. Sodium bis(2-methoxyethoxy)-aluminum hydride solution (Red-Al, 19.8 g, 98.0 mmol) was dissolved in 160 mL of diethyl ether in a 500 mL round bottom flask. F8H6IOH (30 g, 46.4 mmol) was dissolved in 80 mL of diethyl ether and added to the Red-Al solution. The reaction was performed for 3 h at room temperature and then quenched with 200 mL of 2 M HCl solution. The organic phase was washed with 200 mL of brine, followed by drying with magnesium sulfate. The solution was concentrated under reduced pressure and the semifluorinated hexanol (F8H6OH) was recovered by further drying under reduced pressure for 24 h at room temperature. F8H6OH (22.5 g, 43.3 mmol) and CBr_4 (23 g, 69.3 mmol) were dissolved in 100 mL of anhydrous THF in a 500 mL round bottom flask. The mixture was cooled to −5 °C. Triphenyl phosphine (18.1 g, 69.3 mmol) was then added and the reaction was performed for 1 h at −5 °C, followed by an additional 8 h at room temperature. The tetrahydrofuran was then evaporated under reduced pressure and 200 mL of diethyl ether was added to the crude product. The triphenylphosphine oxide byproduct was separated by filtration, and the product was further purified by passing the reaction solution through a short silica gel column to absorb the residual triphenylphosphine oxide using anhydrous methylene chloride as a running solvent (82% yield). 1H NMR ($CDCl_3$, δ in ppm) 3.45 (2H,

Scheme 1. Synthesis of Semifluorinated-Quaternized Triblock Copolymer (SQTC-F8H6Br−H6Br)

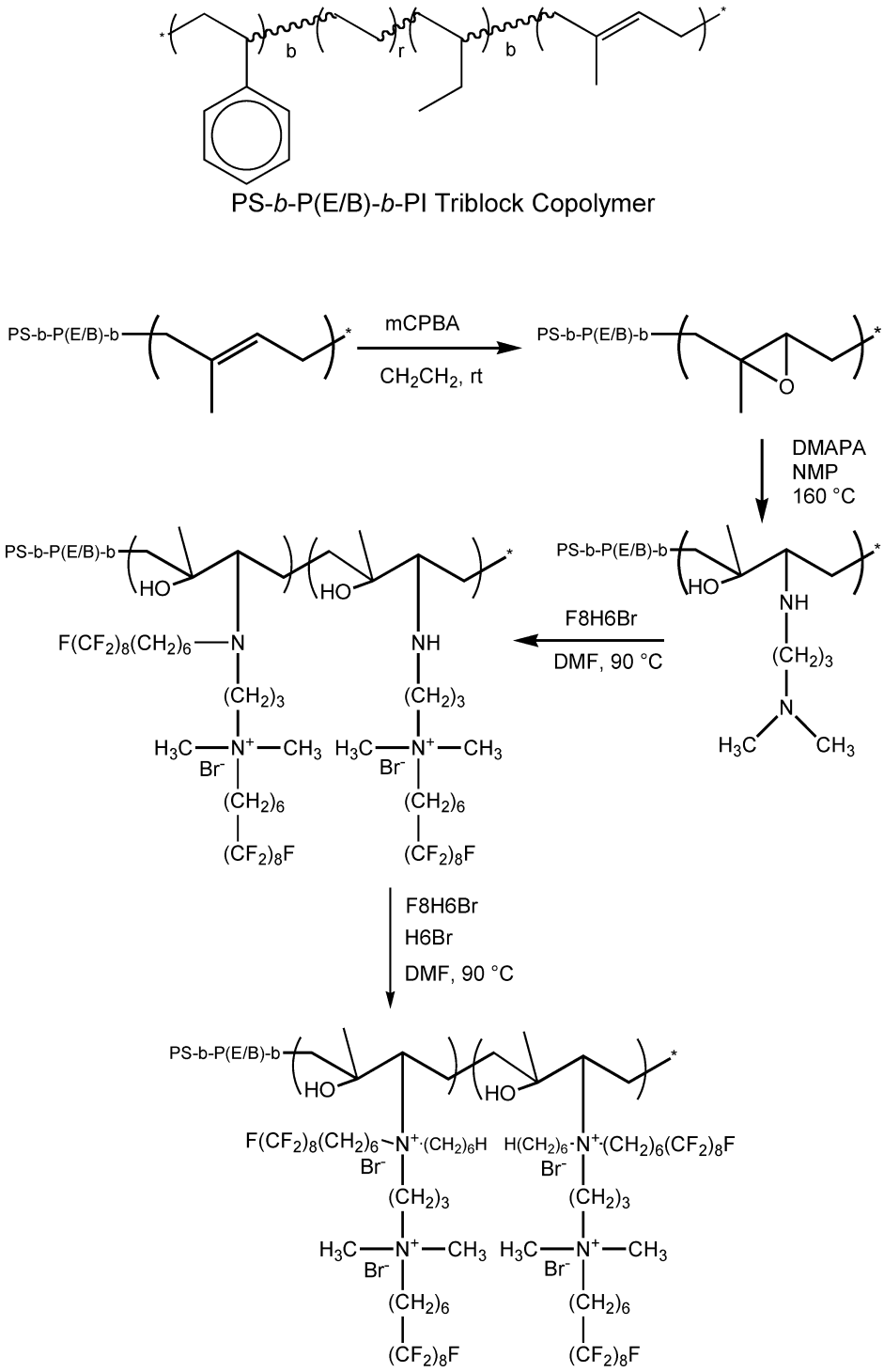

CH_2Br), 2.06 (2H, CF_2CH_2), 1.88 (2H, CH_2CH_2Br), 1.65 (2H, $CF_2CH_2CH_2$), 1.40 (4H, $CF_2CH_2CH_2CH_2CH_2$).

Epoxidation of PS-*b*-P(E/B)-*b*-PI. The modification of the starting triblock copolymer is outlined in Scheme 1. PS-*b*-P(E/B)-*b*-PI, (10 g, 50 mmol of isoprene) was dissolved in 200 mL of methylene chloride in a 500 mL round bottom flask at room temperature. *m*-Chloroperoxybenzoic acid (*m*CPBA) (10.4 g, 60 mmol) was added, and the epoxidation was performed for 8 h at room temperature. About 80 % of the reaction solvent was evaporated under reduced pressure and the epoxidized polymer was precipitated in excess methanol, filtered, dissolved in 30 mL of methylene chloride, re-precipitated in excess methanol, filtered, and dried under reduced pressure at room temperature for 48 h.

Amination of Epoxidized PS-*b*-P(E/B)-*b*-PI. Epoxidized PS-*b*-P(E/B)-*b*-PI (1 g, 4 mmol of epoxy) was dissolved in 50 mL of NMP in a 300 mL round bottom flask at 90 °C. DMAPA (12.3 g, 120 mmol) and TPP (0.2 g, 0.8 mmol) were added and the amination was performed for 48 h at 160 °C under reflux. The aminated block copolymer was precipitated in excess distilled water, filtered, dissolved in 50 mL of NMP, re-precipitated in excess distilled water, filtered, and dried under reduced pres-

sure at room temperature for 48 h. Elemental anal.: C (76.9 %), H (11.6 %), O (5.49 %), N (5.74 %).

Quaternization of Aminated PS-*b*-P(E/B)-*b*-PI with Semifluorinated Hexylbromide (F8H6Br) and Hexylbromide (H6Br). Aminated PS-*b*-P(E/B)-*b*-PI (0.4 g, 5.95 mmol of reactive amino and amine groups) was dissolved in 20 mL of DMF in a 100 mL round bottom flask at 90 °C. F8H6Br (10.4 g, 17.9 mmol) and potassium carbonate (1.38 g, 10 mmol) were added to the reaction mixture. The flask was sealed with a rubber septum and the quaternization reaction was performed for 48 h at 90 °C under a nitrogen atmosphere. The residual amine groups were further quaternized with excess H6Br for 24 h at 90 °C. Following completion of the second quarternization, about 80 % of DMF was removed using a rotary evaporator at reduced pressure. The SQTCs were precipitated in excess diethyl ether, filtered, dissolved in 5 mL of DMF, re-precipitated in excess diethyl ether, filtered, and dried under reduced pressure at room temperature for 48 h. Elemental anal.: C (48.8 %), H (5.6 %), N (2.2 %), F (35.3 %) for first quaternization (SQTC-F8H6Br); C (50.1 %), H (6.1%), N (1.6 %), F (33.1 %) for second quaternization (SQTC-F8H6Br-H6Br).

Polymer and Surface Characterizations. The polymer films for IR spectra of polymers were formed on salt plates and the spectra were obtained using a Mattson 2020 Galaxy Series FTIR spectrometer. The elemental analyses for C, H, N, and F of polymers were performed by Quantitative Technologies, Inc. (QTI).

All samples for surface characterization were prepared by spin coating polymer solutions (3%, w/v) in chloroform on silicon wafers using a spin coater at 1500 rpm for 30 seconds. The surfaces were annealed at 60 °C for 3 days under a vacuum, followed by an additional 12 h at 120 °C.

XPS measurements were performed using a Kratos Axis Ultra Spectrometer (Kratos Analytical, Manchester, UK) with a monochromatic Al Kα X-ray source (1486.6 eV) operating at 225 W under a vacuum of 1.0×10^{-8} Torr. Charge compensation was carried out by injection of low-energy electrons into the magnetic lens of the electron spectrometer. The pass energy of the analyzer was set at 40 eV for high-resolution spectra and 80 eV for survey scans, with energy resolutions of 0.05 and 1 eV, respectively. The spectra were analyzed using CasaXPS v.2.3.12Dev4 software. The C−C peak at 285 eV was used as the reference for binding energy calibration.

NEXAFS experiments were performed using the U7A NIST/Dow materials characterization end-station at the National Synchrotron Light Source at Brookhaven National Laboratory. The X-ray beam was elliptically polarized (polarization factor = 0.85), with the electric field vector dominantly in the plane of the storage ring. The photon flux was about 1×10^{11} photons per second at a typical storage ring current of 500 mA. A spherical grating monochromator was used to obtain monochromatic soft X-rays at an energy resolution of 0.2 eV. The C 1s NEXAFS spectra were acquired for incident photon energy in the range 270−320 eV. The angle of incidence of the X-ray beam, measured from the sample surface, was 50°. A channeltron electron multipier with an adjustable entrance grid bias (EGB) was used to collect the Auger electron partial-electron-yield (PEY) signal resulting from filling of the holes created in the C 1s level. All the data reported here are for a grid bias of −150 V so that the effective Auger electron escape depth is about 2.4 nm (40). The channeltron PEY detector was positioned at an angle of 36° with respect to the incoming X-ray beam and in the equatorial plane of the sample chamber.

Antibacterial Tests.

Cell Growth. Trypticase Soy Broth (TSB, 5 mL; per liter: 3 g of soy meal peptone, 17 g of casein peptone, 2.5 g of glucose, 5 g of NaCl, and 2.5 g of dipotassium hydrogen phosphate) was inoculated with 100 μL of an overnight culture of *S. aureus*, and incubated at 37 °C for 4 h. The cells were centrifuged at 5000 rpm for 1 min using a microcentrifuge (Eppendorf 5415C), and the pellet was resuspended in 1 mL of sterile filtered water.

Colony Counts. Aqueous suspensions of *S. aureus* with concentrations of $\sim 10^6$ cells/mL were sprayed on the test surfaces, dried in air for 2 min and placed in sterile Petri dishes. The test surfaces were prepared by spray-coating of the solutions of SQTCs in chloroform (1.5 %, w/v) on glass slides using a Badger 250 airbrush with 50 psi nitrogen gas flow. To control aerosols, spraying was performed in a class II type A biological safety cabinet (SterilGARD Hood, Baker Company) with a HEPA filter. The sprayed surfaces were covered by molten agar-containing TSB (1.5 % w/v of agar), allowed to solidify and then incubated at 37 °C overnight. The number of bacterial colonies was counted using a colony counter.

LIVE/DEAD *Bac*Light Bacterial Viability Assay. LIVE/DEAD *Bac*Light bacterial viability kit was obtained from Molecular Probes, Inc. Equal volumes of SYTO 9 and propidium iodide were mixed thoroughly in a microcentrifuge tube. The BacLight dye mixture (30 μL) was added to 1 mL of the cell suspension, which was then sprayed on the test surfaces. Immediately after the spraying, the test surfaces were covered with glass coverslips, sealed with fingernail polish to avoid dessication, and incubated in the dark for 15 min. Phase-contrast and fluorescence microscopy were performed, within 1 h after spraying, using an Olympus BX61 epifluorescence microscope with a 100× UPlanApo (N.A.135) objective. The microscope was equipped with filter cubes for viewing SYTO 9 and PI fluorescence. Glass microscope slides were used as controls.

Surface Coatings. Glass slides for biofouling assays with algae were prepared by the same procedure reported in Krishnan *et al.* (14). Glass microscope slides coated with a polydimethylsiloxane elastomer (PDMSe), Silastic® T2 (Dow Corning) prepared as described in ref 41 and polystyrene-*b*-poly (ethylene-*ran*-butylene)-*b*-polystyrene (SEBS, Kraton G1652) were used as standards. The PDMSe standard was included because of its known fouling release properties for macrofouling organisms including *Ulva*. Multilayer surfaces for bioassays were prepared in a manner analogous to that reported in Krishnan et al. (14). SEBS base layers were prepared in the manner previously described. The solutions of SQTCs in chloroform (1.5 %, w/v) were spray-coated on the prepared SEBS-coated glass slides using a Badger 250 airbrush with 50 psi nitrogen gas flow. The surfaces were annealed under a vacuum at 60 °C for 3 days, followed by an additional 12 h at 120 °C.

Settlement of Zoospores and Strength of Attachment of Sporelings of *Ulva*. Nine replicate test samples were leached in a 30 L tank of recirculating deionized water at ~20 °C for 3 days. The slides were equilibrated in artificial seawater 1 h prior to the start of the experiments. Zoospores were released from fertile plants of *Ulva linza* and prepared for assay as described previously (42). Ten milliliters of zoospore suspension (1×10^6 spores per mL), were pipetted into 9 compartments of Quadriperm polystyrene culture dishes (Greiner Bio-One), each containing a test slide. The test slides were incubated in the dark at ~20 °C for 1 h and washed in seawater to remove zoospores that had not settled. Three replicates were used to quantify the density of zoospores attached to the surfaces (43). Sporelings (young plants) were cultured on 6 replicates of each coating (44). Spores were allowed to settle as described above. After washing, the samples were transferred to dishes containing nutrient enriched seawater for 7 days. Growth was estimated by direct measurement of fluorescence from chlorophyll contained within the chloroplasts of the sporelings (young plants) using a Tecan plate reader (GENios Plus) (45). Fluorescence was recorded as Relative Fluorescence Units (RFU) from direct readings. The slides (6 replicates) were read from the top, 300 readings per slide, taken in blocks of 30 × 10. The strength of attachment of the sporelings was determined by jet washing using a water jet (46). The range of impact pressures used was chosen to

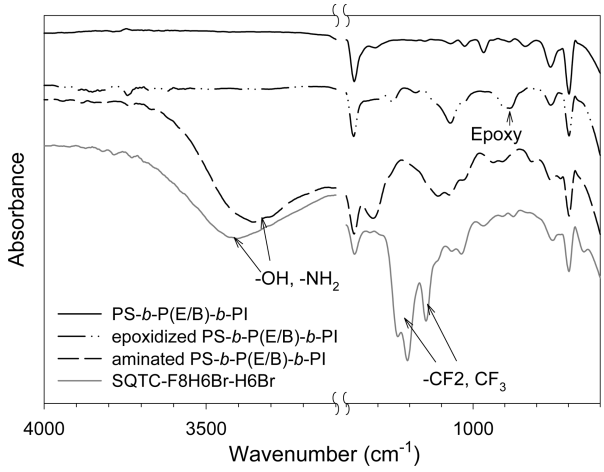

FIGURE 1. FT-IR spectra of PS-*b*-P(E/B)-*b*-PI, epoxidized PS-*b*-P(E/B)-*b*-PI, aminated PS-*b*-P(E/B)-*b*-PI, and SQTC-F8H6Br−H6Br.

provide maximum information on the strength of attachment of the sporelings. RFU readings (80 per slide) were taken from the central part of the slide that was exposed to the water jet. Percentage removal was calculated from the mean RFU reading before and after exposure to the water jet.

Settlement and Attachment Strength of the Diatom, *Navicula.* *Navicula* cells were cultured in F/2 medium contained in 250 mL conical flasks. After 3 days, the cells were in log phase growth. Cells were washed 3 times in fresh medium before harvesting and diluted to give a suspension with a chlorophyll *a* content of approximately 0.25 μg mL^{-1}. Cells were settled in individual dishes containing 10 mL of suspension at ~20°C on the laboratory bench. After 2 h, the slides were gently washed in seawater to remove cells that had not attached (submerged wash). Slides were fixed using 2.5 % glutaraldehyde in seawater. The density of cells attached to the surface was counted on each of 3 replicate slides using an image analysis system attached to a fluorescent microscope. Counts were made for 30 fields of view (each 0.064 mm^2) on each slide.

Three further replicate slides settled with *Navicula* were exposed to a shear stress of 23 Pa (2.02 L s^{-1}) in a water channel. The number of cells remaining attached was counted using the image analysis system described above. Percentage removal was calculated as above.

RESULTS AND DISCUSSION

Synthesis of SQTCs and Characterization. Figure 1 shows the IR spectra of PS-*b*-P(E/B)-*b*-PI, epoxidized PS-*b*-P(E/B)-*b*-PI, aminated PS-*b*-P(E/B)-*b*-PI, and SQTC-F8H6Br−H6Br. All IR spectra show the C−H bending vibrations associated with the styrene phenyl ring at 700 cm^{-1}. After the epoxidation reaction, an absorption peak, which indicates the presence of the epoxy groups, was observed between 875−900 cm^{-1}. This epoxy peak disappeared after the 48 h amination with DMAPA at 160 °C, whereas the strong stretching vibration of amine and hydroxyl were present around 3300−3600 cm^{-1} implying that the epoxy groups were consumed by the amination. Based on the NMR analysis (data is not shown) all double bonds from the isoprene block disappeared indicating 100 % epoxidation. Using elemental analysis, it was determined that the aminated PS-*b*-P(E/B)-*b*-PI contained 5.7 wt % nitrogen content, corresponding to 59.6 mol % amination based on the number of 245 epoxy groups present in the epoxidized PS-*b*-P(E/B)-*b*-PI. The quaternization reaction with F8H6Br and H6Br resulted in the appearance of C−F stretching resonance at 1100−1300 cm^{-1} indicating the attachment of semifluorinated groups (14, 47).

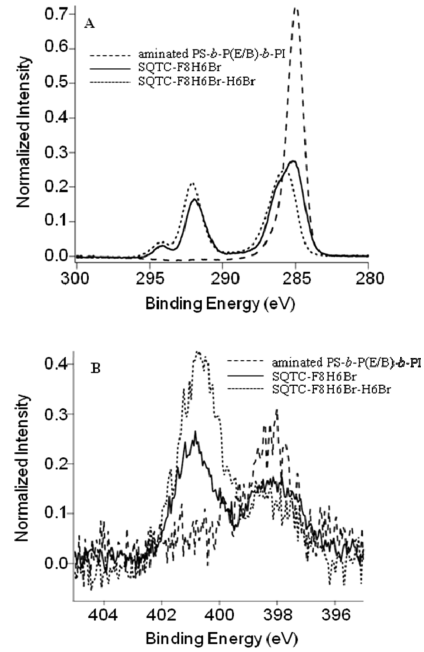

FIGURE 2. (A) C 1s and (B) N 1s XPS spectra of the surfaces of aminated PS-*b*-P(E/B)-*b*-PI, SQTC-F8H6Br, and SQTC-F8H6Br−H6Br.

X-ray Photoelectron Spectroscopy. Figure 2A shows high-resolution carbon 1s XPS spectra of aminated PS-*b*-P(E/B)-*b*-PI, SQTC-F8H6Br, and SQTC-F8H6Br−H6Br. The spectra are normalized so that the total area under the carbon peaks was equal to unity. The aminated PS-*b*-P(E/B)-*b*-PI showed strong intensity peaks of C═C and C−C near 285 eV. The surface of SQTC-F8H6Br quaternized with semifluorinated hexylbromide, $F(CF_2)_8(CH_2)_6Br$, showed distinct $-CF_2-$ and $-CF_3$ peaks near 292 and 294 eV, respectively. The lowered intensity of the peaks associated with C═C and C−C combined with the appearance of $-CF_2-$ and $-CF_3$ peaks is evidence of the attachment of fluorinated side chains through the quaternization with F8H6Br. The further reaction by addition of H6Br resulted not only in a slight decrease in the C═C and C−C peak intensities but also a small increase in $-CF_2$- and $-CF_3$ peak intensities. This suggests that the added hexyl groups make the surface more hydrophobic causing additional surface reconstruction that led to the slight increase in the $-CF_2-$ and $-CF_3$. Figure 2B shows the N 1s XPS spectra of the polymer before and after the quaternization reaction with F8H6Br, followed by quaternization with H6Br. The quaternization reaction resulted in the shift of the nitrogen peak near 398 eV, which corresponds to unquaternized nitrogen, to a higher binding energy near 400.5 eV, corresponding to quaternized nitrogen. The fraction of quaternized nitrogen atoms present in SQTC-F8H6Br and SQTC-F8H6Br-H6Br, calculated by comparing the areas under the two peaks, are 45 and 70%, respectively.

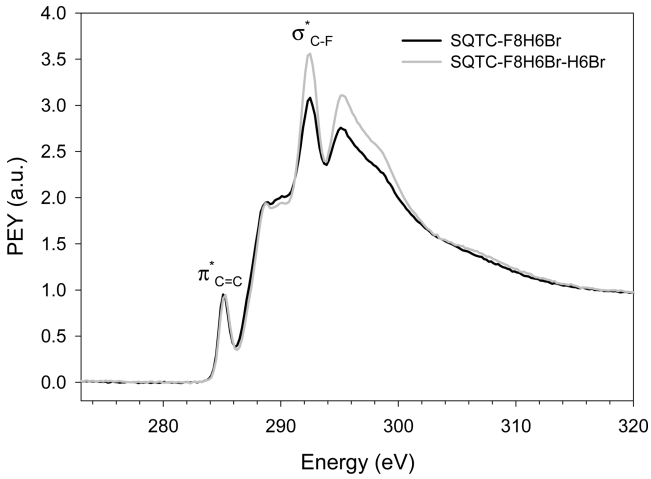

FIGURE 3. Normalized C 1s NEXAFS spectra of the surfaces at an angle of 50° between the X-ray beam and the surface of SQTC-F8H6Br and SQTC-F8H6Br−H6Br. The spectra are normalized by scaling them so that the PEY post-edge signal at 320 eV is equal to 1.

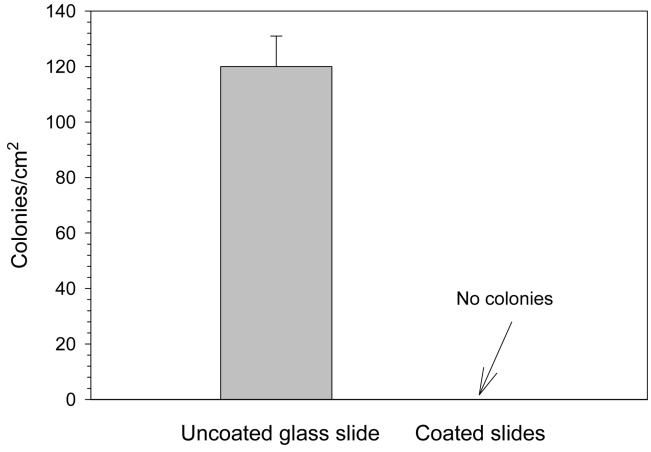

FIGURE 4. Antibacterial activities of SQTC-F8H6Br-H6Br against *S. aureus*.

NEXAFS Analysis of the Surfaces. Figure 3 shows the normalized C 1s NEXAFS spectra of spin-coated surfaces of SQTC-F8H6Br and SQTC-F8H6Br−H6Br. The characteristic C 1s → $\pi^*_{C=C}$ signals derived from the polystyrene block were observed near 285 eV for all spectra. The characteristic C 1s → σ^*_{C-F} signal near 293 eV can be seen in the NEXAFS spectra of SQTC-F8H6Br and SQTC-F8H6Br-H6Br. The intensity of C 1s → σ^*_{C-F} of SQTC-F8H6Br-H6Br is higher than that of SQTC-F8H6Br due to the surface reconstruction after introduction of hydrophobic hexyl groups, which is in good agreement with XPS analysis.

Antibacterial Behavior of SQTC-F8H6Br-H6Br against *S. aureus*. The antibacterial activity of SQTC-F8H6Br-H6Br was determined by comparing the number of bacterial colonies of *S. aureus* grown on coated test surfaces relative to uncoated glass slides. As shown in Figure 4, the mean value of bacterial colonies of *S. aureus* grown on uncoated glass slides after overnight incubation was ca. 125 colonies/cm^2. In contrast, no colonies formed on surfaces coated with SQTC-F8H6Br-H6Br, which indicates high antibacterial activity. The further study by LIVE/DEAD *Bac*Light bacterial viability assay gave more information regarding the antibacterial behavior of SQTC-F8H6Br-H6Br surface on *S. aureus*.

Figure 5 shows the fluorescence microscopy images of the LIVE/DEAD assay after 45 min contact of bacterial cells with the test surfaces. Figure 6 depicts the percentage of dead cells determined by comparison of the live cells (green) and dead cells (red). At first, the images on *S. aureus* showed no discernable difference between control and coated surfaces (Figure 5A,B). However, analysis of the images for total fluorescence by software (Slidebook software, Intelligent Imaging Inc.) showed that more cells (ca. 2 fold) were dead on the SQTC-coated surfaces. There were no significant changes in the relative number of dead cells over a period of 1 h (Figure 6), indicating that most of the non-viable cells had been dead within the first 15 min of contact. This result is quite different from the previous study by Krishnan et al. (14). In that study, surfaces of semifluorinated quaternized polystyrene-*block*-poly-(4-vinyl pyridine) PS-*b*-P4VP block copolymers showed almost 100 % bactericidal activity against *S. aureus*. One of the possible approaches to explain

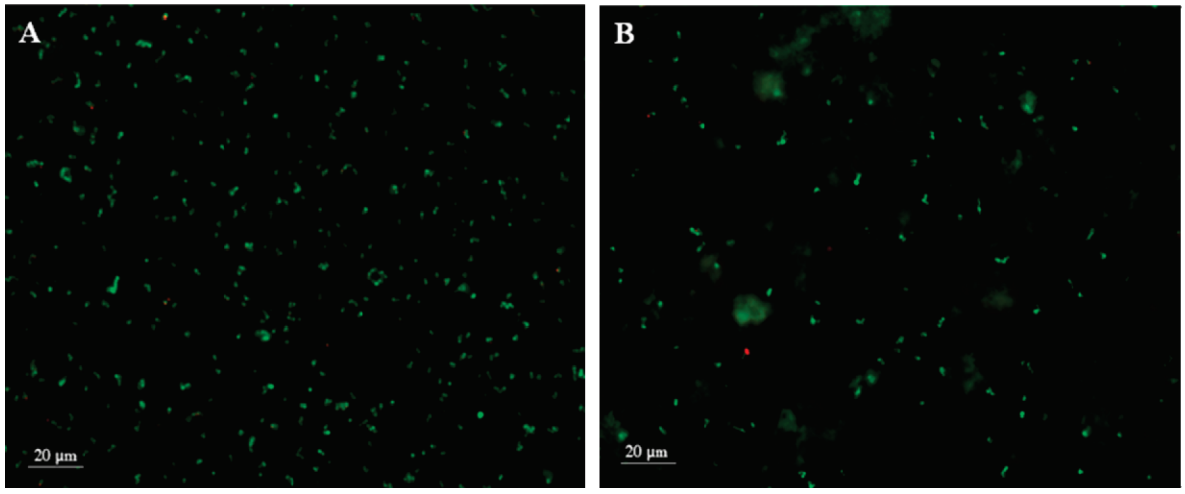

FIGURE 5. Images of *S. aureus* on (A) glass control; (B) SQTC-F8H6Br-H6Br coated surfaces by LIVE/DEAD *Bac*Light bacterial viability assay. Cells with intact cell membranes are stained green, and those with dead ones are stained red. The length of the scale bar is 20 μm.

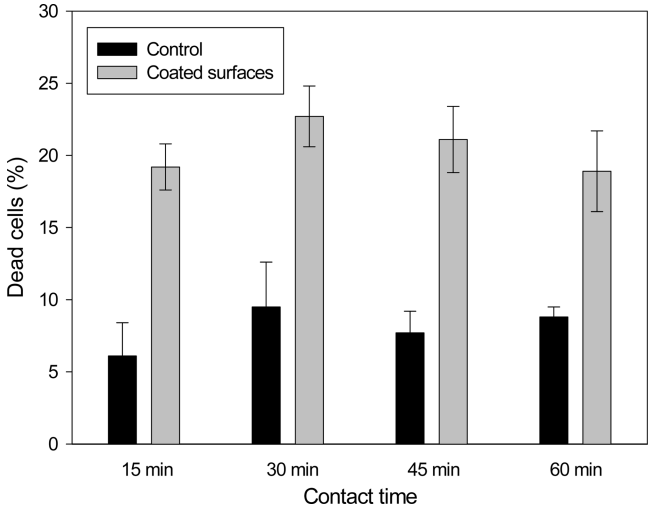

FIGURE 6. Antibacterial behavior of SQTC-F8H6Br−H6Br against *S. aureus* by LIVE/DEAD *Bac*Light bacterial viability assay. Bars show the standard deviation.

the observed difference in antibacterial activity is the relative amount of quaternized nitrogen in each of the polymers. In 1 g of 59.6 % aminated PS-*b*-P(E/B)-*b*-PI, there is 4.0 mmol nitrogen. On the basis of N 1s XPS spectra (Figure 2B), 70 % of this nitrogen was quaternized, which corresponds to 2.8 mmol quaternized nitrogen per 1 g of polymer. Meanwhile, the total amount of quaternized nitrogen in 1 g of PS_{62k}-*b*-$P4VP_{66k}$ is 4.66 mmol. Moreover, the low surface energy poly(ethylene-*ran*-butylene) central block in the semifluorinated quaternized triblock copolymer can also segregate to the surface, lowering the surface concentration of quaternized nitrogen atoms even further. Thus, more quaternized nitrogen on the surfaces seems to act as a favorable factor for enhanced bactericidal activity. We have also studied antibacterial activity against a marine bacterium, Gram-negative *Cobetia marina* (*C. marina*). Because *C. marina* did not attach well to the surfaces tested, we could not obtain antibacterial activity data using colony counting. However, a LIVE/DEAD assay gave us the insight that the coated surfaces possessed antibacterial activity against Gram-negative *C. marina*. We present additional data in supporting information (see Figure S1 in the Supporting Information). The images of *C. marina* showed that more cells on a coated surface were dead compared to cells on a control (see Figure S1A,B in the Supporting Information), and the percentage of dead cells seemed to increase with time, whereas the dead cells on the control surface showe no significant changes (see Figure S1C in the Supporting Information). Thus, the surface of SQTC-F8H6Br-H6Br appears to have antibacterial activity against Gram-negative *C. marina*.

Settlement of Zoospores and Strength of Attachment of Sporelings of *Ulva* to Antimicrobial Coatings. *Ulva* zoospores are motile cells, which lack a cell wall and are approximately 7−8 μm in length. The spores swim using their 4 flagella to propel themselves through the water until a suitable surface for settlement is located. Motility is lost at settlement and the spores adhere through discharge of a glycoprotein adhesive (48) and then rapidly germinate into sporelings (young plants). The density of settled spores

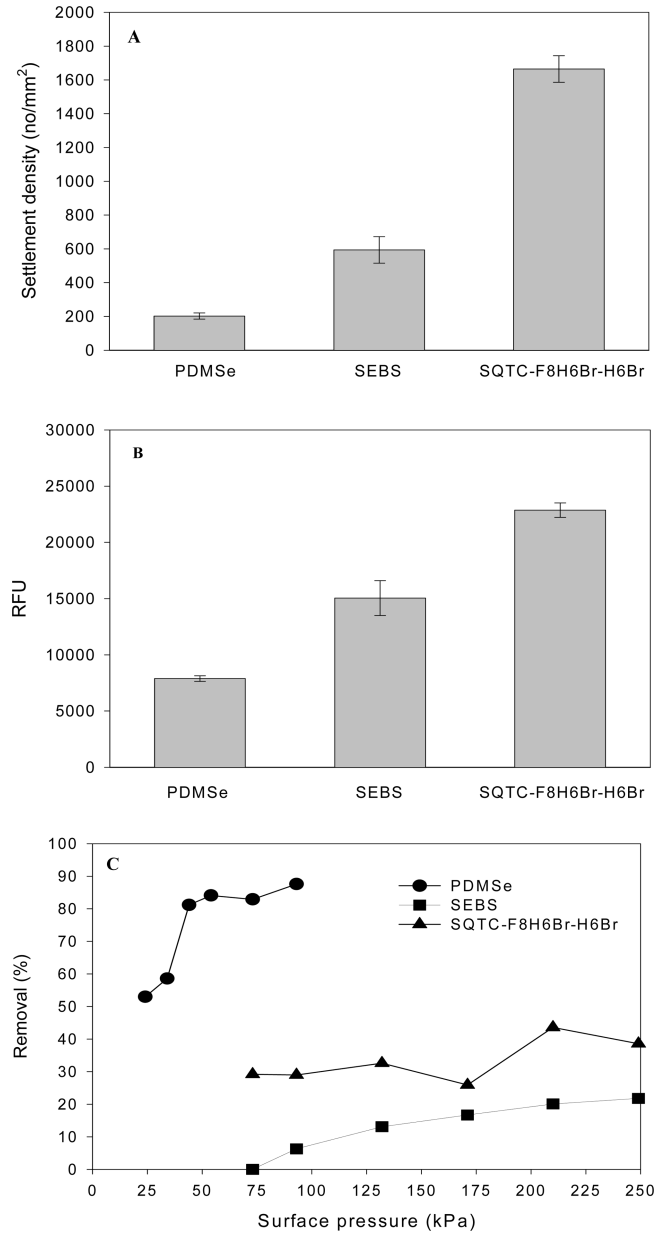

FIGURE 7. (A) Settlement density of *Ulva* zoospores (each point is the mean from 90 counts on 3 replicate slides; bars show 95% confidence limit); (B) biomass of sporelings after 7 days of growth (each point is the mean biomass from 6 replicate slides measured using a fluorescence plate reader; bars show standard error of the mean); and (C) percentage removal of *Ulva* sporelings by a range of impact pressures generated by a water jet on different surfaces.

on SQTC-F8H6Br-H6Br, SEBS, and PDMSe (Figure 7A) shows considerably more spores settled on the quaternized surface than on the PDMSe and SEBS standards.

The biomass of sporelings after 7 days of growth largely reflected the number of spores settled (Figure 7B). However, the length of sporelings on SQTC-F8H6Br-H6Br was less than on the PDMSe standard and the growth form was more stunted (Figure 8). The reason for the lower growth may be due to chronic toxicity mediated by the quaternary ammonium component of the coating, but another explanation is that growth is inhibited by the high density of settled spores competing for space and nutrients.

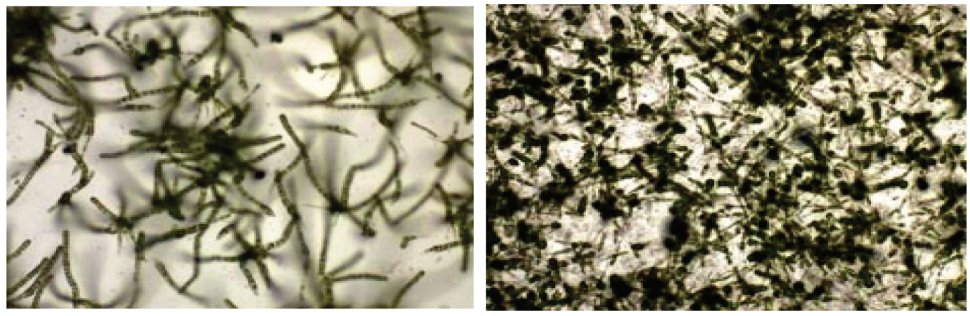

FIGURE 8. Images of sporelings after 7 days of growth on (left) PDMSe standard and (right) SQTC-F8H6Br-H6Br.

The percentage removal of sporelings at a range of pressures generated by a water jet is shown in Figure 7C. Sporelings were removed from the PDMSe standard at low impact pressures reflecting the fouling-release characteristics of this elastomer (14, 45). Removal of sporelings from the SQTC-F8H6Br−H6Br surface and the SEBS required much higher impact pressures. The highest observed removal of sporelings on the SQTC-F8H6Br−H6Br surface was only about 40%, even at 250 kPa, which demonstrates their strong attachment strength to this surface. Fluorinated polymers possess low surface energy and are hydrophobic (49−51), suggesting their possible use as practical antifouling/fouling-release coatings for marine surfaces. The SQTC-F8H6Br-H6Br surface, however, showed the highest settlement of *Ulva* spores despite the relatively high content of fluorine in this material (ca. 33% based on elemental analysis). This suggests that the large amount of N^+ ions from the quaternization reactions caused more spores to settle and adhere to the surfaces due to the electrostatic attraction between positively charged surfaces and negatively charged spores (52), which would be an important property for primary antibacterial action we mentioned earlier. Although sporeling adhesion was stronger on the SQTC surfaces compared to PDMSe, the SQTC surfaces showed higher release compared to the SEBS controls.

Settlement of Diatoms. Diatom cells are not motile in the water column and in this laboratory assay, reach the test surface by gravity. Thus, at the end of the settlement period, a similar number of cells were present on all surfaces (data not shown). The adhesion strength of cells to the test surfaces was quantified by exposing slides to a wall shear stress of 23 Pa. One way analysis of variance on arc-sine transformed data supported by Tukey tests showed that the percentage of cells removed from SQTC-F8H6Br-H6Br was significantly higher than from the SEBS standard ($F_{2, 267} = 15.3$ $P<0.05$). However, there was no significant difference between removal from the SQTC-F8H6Br−H6Br and the PDMSe standard, reflecting the relatively strong attachment of *Navicula* to both PDMSe and SQTC-F8H6Br-H6Br surfaces (Figure 9).

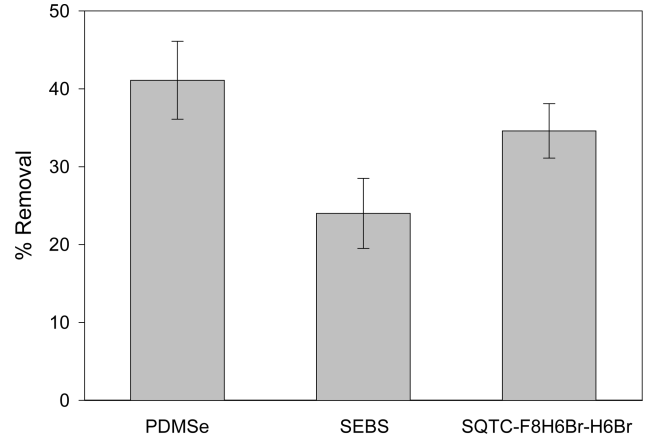

FIGURE 9. The removal of diatoms from different surfaces. Each point is the mean from 90 counts on 3 replicate slides. Bars show 95% confidence limits from arc-sine transformed data.

CONCLUSIONS

Semifluorinated-quaternized triblock copolymers (SQTCs) were synthesized by the quaternization reaction of semifluorinated hexylbromide with aminated polystyrene-*block*-poly(ethylene-*ran*-butylene)-*block*-polyisoprene triblock copolymer. Characteristic $-CF_2-$ peak and $1s \rightarrow \sigma^*_{C-F}$ resonance peaks in the XPS and NEXAFS spectra, respectively, confirmed the presence of semifluorinated alkyl groups, which are directly attached to nitrogen atoms of the aminated block, at the surfaces. XPS measurements of N 1s showed 70 % of the nitrogen was quaternized by the reactions with F8H6Br and H6Br. Antibacterial experiments by colony counting and LIVE/DEAD *Bac*Light bacterial viability assay showed that the surfaces of SQTCs were highly antibacterial against airborne *S. aureus* with >99 % inhibition. However, the SQTC surfaces did not exhibit strong algicidal activity against the marine algae, but showed weaker adhesion than the SEBS controls. A large number of N^+ sites, promoting electrostatic attraction, is the likely reason for the high number of *Ulva* spores that settled on and adhered to the surface. Thus, although these surfaces did demonstrate very impressive antibacterial character, they did not appear to show promise as either marine antifouling or fouling-release coatings.

Acknowledgment. This work was supported by United States Department of Defense's Strategic Environmental Research and Development Program (SERDP), Grant WP #1454 with additional support from the Office of Naval Research (ONR) through award # N00014-05-1-0134 (J.A.C. and M.E.C.) and N00014-02-1-0170 (C.K.O. and E.J.K.). K.E.S. and E.J.K. acknowledge partial support from an NSF Graduate Fellowship and the NSF Polymers Program (DMR-0704539) as well as the use of facilities funded by the NSF-MRSEC program (UCSB MRL, DMR-0520415).

Supporting Information Available: Cell culture of Gram-negative *C. maria* and antibacterial activity by LIVE/DEAD *Bac*Light bacterial viability assay (PDF). This material is available free of charge via the Internet at http://pubs.acs.org.

REFERENCES AND NOTES

(1) Nonaka, T.; Noda, E.; Kurihara, S. *J. Appl. Polym. Sci.* **2000**, *77*, 1077–1086.
(2) Li, G. J.; Shen, J. R.; Zhu, Y. L. *J. Appl. Polym. Sci.* **2000**, *78*, 668–675.
(3) Tashiro, T. *Macromol. Mater. Eng.* **2001**, *286*, 63–87.
(4) Levy, S. B. *Emerging Infect. Dis.* **2001**, *7*, 512–515.
(5) Sauvet, G.; Dupond, S.; Kazmierski, K.; Chojnowski, J. *J. Appl. Polym. Sci.* **2000**, *75*, 1005–1012.
(6) Shin, Y.; Yoo, D. I.; Min, K. *J. Appl. Polym. Sci.* **1999**, *74*, 2911–2916.
(7) Silver, S.; Phung, L. T.; Silver, G. *J. Ind. Microbiol. Biotechnol.* **2006**, *33*, 627–634.
(8) Lala, N. L.; Ramaseshan, R.; Li, B. J.; Sundarrajan, S.; Barhate, R. S.; Liu, Y. J.; Ramakrishna, S. *Biotechnol. Bioeng.* **2007**, *97*, 1357–1365.
(9) Jain, P.; Pradeep, T. *Biotechnol. Bioeng.* **2005**, *90*, 59–63.
(10) Grunlan, J. C.; Choi, J. K.; Lin, A. *Biomacromolecules* **2005**, *6*, 1149–1153.
(11) Dizman, B.; Elasri, M. O.; Mathias, L. J. *Macromolecules* **2006**, *39*, 5738–5746.
(12) Huang, J. Y.; Murata, H.; Koepsel, R. R.; Russell, A. J.; Matyjaszewski, K. *Biomacromolecules* **2007**, *8*, 1396–1399.
(13) Kenawy, E. R. *J. Appl. Polym. Sci.* **2001**, *82*, 1364–1374.
(14) Krishnan, S.; Ward, R. J.; Hexemer, A.; Sohn, K. E.; Lee, K. L.; Angert, E. R.; Fischer, D. A.; Kramer, E. J.; Ober, C. K. *Langmuir* **2006**, *22*, 11255–11266.
(15) Kurt, P.; Wood, L.; Ohman, D. E.; Wynne, K. J. *Langmuir* **2007**, *23*, 4719–4723.
(16) Cheng, Z. P.; Zhu, X. L.; Shi, Z. L.; Neoh, K. G.; Kang, E. T. *Ind. Eng. Chem. Res.* **2005**, *44*, 7098–7104.
(17) Chen, C. Z. S.; Beck-Tan, N. C.; Dhurjati, P.; van Dyk, T. K.; LaRossa, R. A.; Cooper, S. L. *Biomacromolecules* **2000**, *1*, 473–480.
(18) Park, D.; Wang, J.; Klibanov, A. M. *Biotechnol. Prog.* **2006**, *22*, 584–589.
(19) Hu, F. X.; Neoh, K. G.; Cen, L.; Kang, E. T. *Biotechnol. Bioeng.* **2005**, *89*, 474–484.
(20) Lin, J.; Qiu, S. Y.; Lewis, K.; Klibanov, A. M. *Biotechnol. Bioeng.* **2003**, *83*, 168–172.
(21) Kawabata, N.; Fujita, I.; Inoue, T. *J. Appl. Polym. Sci.* **1996**, *60*, 911–917.
(22) Goodson, B.; Ehrhardt, A.; Ng, S.; Nuss, J.; Johnson, K.; Giedlin, M.; Yamamoto, R.; Moos, W. H.; Krebber, A.; Ladner, M.; Giacona, M. B.; Vitt, C.; Winter, J. *Antimicrob. Agents. Chemother.* **1999**, *43*, 1429–1434.
(23) Dizman, B.; Elasri, M. O.; Mathias, L. J. *J. Appl. Polym. Sci.* **2004**, *94*, 635–642.
(24) Scharff, T. G.; Maupin, W. C. *Biochem. Pharmacol.* **1960**, *5*, 79–86.
(25) Wyatt, J. M.; Knowles, C. J. *Int. Biodeterior. Biodegrad.* **1995**, *35*, 227–248.
(26) Tiller, J. C.; Lee, S. B.; Lewis, K.; Klibanov, A. M. *Biotechnol. Bioeng.* **2002**, *79*, 465–471.
(27) Tiller, J. C.; Liao, C. J.; Lewis, K.; Klibanov, A. M. *Proc. Natl Acad. Sci. U.S.A.* **2001**, *98*, 5981–5985.
(28) Nho, Y. C.; Park, J. S.; Jin, J. H. *J. Macromol. Sci., Part A: Pure Appl. Chem.* **1997**, *A34*, 831–842.
(29) Townsin, R. L. *Biofouling* **2003**, *19*, 9–15.
(30) Schultz, M. P. *Biofouling* **2007**, *23*, 331–341.
(31) Jelic-Mrcelic, G.; Sliskovic, M.; Antolic, B. *Biofouling* **2006**, *22*, 293–302.
(32) Genzer, J.; Efimenko, K. *Biofouling* **2006**, *22*, 339–360.
(33) Kavanagh, C. J.; Quinn, R. D.; Swain, G. W. *J. Adhes.* **2005**, *81*, 843+.
(34) Wendt, D. E.; Kowalke, G. L.; Kim, J.; Singer, I. L. *Biofouling* **2006**, *22*, 1–9.
(35) Beigbeder, A.; Degee, P.; Conlan, S. L.; Mutton, R. J.; Clare, A. S.; Pettitt, M. E.; Callow, M. E.; Callow, J. A.; Dubois, P. *Biofouling* **2008**, *24*, 291–302.
(36) Brady, R. F.; Bonafede, S. J.; Schmidt, D. L. *JOCCA Surf. Coat. Int.* **1999**, *82*, 582–585.
(37) Gan, D. J.; Mueller, A.; Wooley, K. L. *J. Polym. Sci., Part A: Polym. Chem.* **2003**, *41*, 3531–3540.
(38) Youngblood, J. P.; Andruzzi, L.; Ober, C. K.; Hexemer, A.; Kramer, E. J.; Callow, J. A.; Finlay, J. A.; Callow, M. E. *Biofouling* **2003**, *19*, 91–98.
(39) Majumdar, P.; Lee, E.; Patel, N.; Ward, K.; Stafslien, S. J.; Daniels, J.; Chisholm, B. J.; Boudjouk, P.; Callow, M. E.; Callow, J. A.; Thompson, S. E. M. *Biofouling* **2008**, *24*, 185–200.
(40) Genzer, J.; Kramer, E. J.; Fischer, D. A. *J. Appl. Phys.* **2002**, *92*, 7070–7079.
(41) Schumacher, J. F.; Carman, M. L.; Estes, T. G.; Feinberg, A. W.; Wilson, L. H.; Callow, M. E.; Callow, J. A.; Finlay, J. A.; Brennan, A. B. *Biofouling* **2007**, *23*, 55–62.
(42) Callow, M. E.; Callow, J. A.; Pickett-Heaps, J. D.; Wetherbee, R. *J. Phycol.* **1997**, *33*, 938–947.
(43) Callow, M. E.; Jennings, A. R.; Brennan, A. B.; Seegert, C. E.; Gibson, A.; Wilson, L.; Feinberg, A.; Baney, R.; Callow, J. A. *Biofouling* **2002**, *18*, 237–245.
(44) Chaudhury, M. K.; Finlay, J. A.; Chung, J. Y.; Callow, M. E.; Callow, J. A. *Biofouling* **2005**, *21*, 41–48.
(45) Casse, F.; Ribeiro, E.; Ekin, A.; Webster, D. C.; Callow, J. A.; Callow, M. E. *Biofouling* **2007**, *23*, 267–276.
(46) Finlay, J. A.; Callow, M. E.; Schultz, M. P.; Swain, G. W.; Callow, J. A. *Biofouling* **2002**, *18*, 251–256.
(47) Lamperti, A.; Ossi, P. M. *Appl. Surf. Sci.* **2003**, *205*, 113–120.
(48) Callow, J. A.; Callow, M. E. *Biol. Adhes.* **2006**, 63–78.
(49) Wang, J. G.; Ober, C. K. *Macromolecules* **1997**, *30*, 7560–7567.
(50) Krishnan, S.; Kwark, Y. J.; Ober, C. K. *Chem. Rec.* **2004**, *4*, 315–330.
(51) Almeida, E.; Diamantino, T. C.; de Sousa, O. *Prog. Org. Coat.* **2007**, *59*, 2–20.
(52) Ederth, T.; Nygren, P.; Pettitt, M. E.; Ostblom, M.; Du, C. X.; Broo, K.; Callow, M. E.; Callow, J.; Liedberg, B. *Biofouling* **2008**, *24*, 303–312.

AM900748V